Early prediction of tumor response to treatment : pre-clinical validation of ^{99m}Tc-duramycin

Journal of Nuclear Medicine, published on February 2, 2016 as doi:10.2967/jnumed.115.168344

Early prediction of tumor response to treatment: pre-clinical validation of ^{99m}Tc-duramycin

Filipe Elvas*[1,2], Christel Vangestel[1,2], Koon Pak[3], Peter Vermeulen[4], Brian Gray[3], Sigrid Stroobants[1,2], Steven Staelens[1], Leonie wyffels[1,2]

[1]Molecular Imaging Center Antwerp, University of Antwerp, Wilrijk, Belgium; [2]University Hospital Antwerp, Department of Nuclear Medicine, Edegem, Belgium; [3]Molecular Targeting Technologies, Inc., Pennsylvania, USA; [4]Laboratory of Pathology, General Hospital Sint-Augustinus, Antwerp, Belgium

For correspondence or reprints contact: Leonie wyffels, Department of Nuclear Medicine, University Hospital Antwerp, Wilrijkstraat 10, 2650 Edegem, Belgium.

Email: leonie.wyffels@uza.be

Telephone number: +3238215699

Fax number: +3238253308

*Filipe Elvas, PhD student

Department of Nuclear Medicine, University Hospital Antwerp, Wilrijkstraat 10, 2650 Edegem, Belgium.

Email: filipe.elvas@uantwerpen.be

Telephone number: +3238215692

Fax number: +3238253308

Financial support: GOA (G.0135.13).

SHORT RUNNING TITLE: RESPONSE EVALUATION WITH ^{99m}TC-DURAMYCIN

ABSTRACT

Non-invasive imaging of cell death can provide an early indication of tumor treatment efficacy which will aid clinicians to timely distinguish responding versus non-responding patients. ^{99m}Tc-duramycin is a SPECT tracer for cell death imaging. In this study, we aimed at validating ^{99m}Tc-duramycin for imaging early tumor treatment response. **Methods:** An in vitro binding assay was performed in COLO205 cells treated with 5-FU (3.1, 31 or 310 μM) and oxaliplatin (0.7 or 7 μM) or radiation (2 or 4.5 Gy). ^{99m}Tc-duramycin cell binding and the levels of cell death were evaluated after treatment. In vivo imaging was performed in CD1-/- mice bearing COLO205 human colorectal cancer tumors treated with irinotecan (100 mg/kg), oxaliplatin (5 mg/kg), irinotecan (80 mg/kg) in combination with oxaliplatin (5 mg/kg) or vehicle (0.9% NaCl and 5% glucose; n=6/group). For radiotherapy studies, COLO205 tumors received 4.5 Gy, two fractions of 4.5 Gy in a 24 h interval, pre-treatment with 80 mg/kg irinotecan combined with two fractions of 4.5 Gy in a 24 h interval or no treatment (n=5-6/group). Therapy response was evaluated by ^{99m}Tc-duramycin SPECT 24 h after the last dose of therapy. Blocking was used to confirm tracer specificity. Radiotracer uptake in the tumors was validated ex vivo using γ-counting, cleaved caspase-3 and TUNEL histology. **Results:** Chemo- and radiotherapy treatment increased ^{99m}Tc-duramycin binding to COLO205 cells in a concentration/dose- and time-dependent manner, which was in good correlation with cell death levels ($p<0.05$) as analyzed by annexin V and caspase 3/7 activity. In vivo, ^{99m}Tc-duramycin uptake in COLO205 xenografts was increased 2.3- and 2.8-fold ($p<0.001$), in mice treated with irinotecan and combination therapy, respectively. Blocking with unlabeled duramycin demonstrated specific binding of the radiotracer. After tumor irradiation with 4.5 Gy, ^{99m}Tc-duramycin uptake in tumors increased significantly (1.24 ± 0.07%I.D./g vs. 0.57 ± 0.08%I.D./g in the unirradiated tumors; $p<0.001$). Gamma-counting of radioactivity in the tumors positively correlated with cleaved caspase-3 ($r=0.85$, $p<0.001$) and TUNEL ($r=0.81$, $p<0.001$) staining. **Conclusion:** We demonstrated that ^{99m}Tc-duramycin can be used to image cell death induction early after chemotherapy and

radiotherapy. It holds potential to be translated into clinical assessment of early treatment response.

Key Words: Cell death; ^{99m}Tc-duramycin; SPECT imaging; chemotherapy; radiotherapy.

INTRODUCTION

Objective and accurate evaluation of tumor response to therapy represents one of the biggest challenges in oncology. Tailoring the choice of therapy to the individual patient will help clinicians to match patients with the appropriate therapies, enabling a personalized medicine approach. An early assessment of therapeutic effectiveness will avoid treatment related toxicity to the patient and could lead to improved patient survival by allowing early treatment intensification, discontinuation of ineffective therapy, or initiation of more effective second-line therapy. There is however, a lack of validated biomarkers for treatment response evaluation, despite the active research in this area (reviewed in (*1*)). Currently in clinical practice, the evaluation of response focuses on the volumetric and morphometric changes in the tumor based on the response evaluation criteria in solid tumors (RECIST) (*2*). The major drawback of treatment response evaluation based upon RECIST is that it usually takes a few weeks following treatment before tumor shrinkage becomes apparent. Since molecular events precede gross morphological changes, tumor response assessment based upon the molecular effects of therapy could show superior sensitivity and specificity over anatomical imaging techniques.

Most anti-cancer therapies, such as chemotherapy and radiation therapy, induce tumor cell death through several pathways (*3,4*). Consequently, failure of therapy frequently is a result of resistance against cell death (*5*). At a clinical level, non-invasive imaging of cell death will allow identification of non-responding tumors at an early stage after start of treatment which will lead to a timely change in individualized treatment plan, increasing the probability of response and ultimately patient survival. Non-invasive molecular imaging of therapy-induced cell death can be achieved by using positron emission tomography (PET) or single-photon emission computed tomography (SPECT) radiotracers that specifically target hallmarks of the cell death process. A number of different radiotracers have been developed over the past years targeting specific events of apoptosis (recently reviewed in (*6*)). Existing PET and SPECT tracers for cell

death imaging are targeting externalized aminophospholipids, such as phosphatidylserine (^{99m}Tc-Annexin V, ^{99m}Tc-labelled C2A domain of synaptotagmin I) and phosphatidylethanolamine (PE; ^{99m}Tc-duramycin), apoptotic cell membrane imprint (^{18}F-ML-10) and intracellular caspase-3 activation (^{18}F-ICMT-11, ^{18}F-C-SNAT) during the apoptotic process. Among these, ^{99m}Tc-Annexin V is the most widely studied apoptosis imaging tracer and it has been extensively explored in clinical trials to image treatment-induced cell death in human lung, lymphoma and breast cancer patients (*7*). Nevertheless, ^{99m}Tc-Annexin V failed to reach clinical usefulness due to its slow clearance rate from nontargeted tissues, which contributes to low tumor-to-background ratios (*6*). In this context, the PE binding radiotracer ^{99m}Tc-duramycin has recently gained attention for cell death detection in animal models of disease (*8-10*), exploiting its high affinity and selectivity for PE and optimal biodistribution profile for in vivo SPECT imaging of cell death. Recently, we have demonstrated favorable dosimetry estimates together with the usefulness of ^{99m}Tc-duramycin for the early detection of irinotecan-induced tumor cell death in a proof-of-concept study (*11*).

In the present study, we aimed at further validating the utility of ^{99m}Tc-duramycin for imaging the early response of tumor to various chemotherapy and radiation therapy schemes, with an eye towards the clinical translation of this cell death-targeting SPECT radiotracer. Blocking and ex vivo biodistribution studies were carried out to validate the SPECT data and confirm the specificity of ^{99m}Tc-duramycin to image therapy-induced tumor cell death.

MATERIALS AND METHODS

Radiolabeling of Duramycin

^{99m}Tc-duramycin was prepared by adding 1480 MBq ^{99m}Tc-pertechnetate to a duramycin kit (15 μg) and heating at 80°C for 20 min. The obtained ^{99m}Tc-duramycin was purified using high-performance liquid chromatography as previously described (*11*).

In Vitro Binding Assay

COLO205 human colorectal adenocarcinoma cells (ATCC-CCL-222; Perkin Elmer, Belgium) were grown in complete RPMI1640 medium supplemented with 2 mM L-glutamine, 1 mM sodium pyruvate, 10% fetal bovine serum and 100 U/ml penicillin plus 100 mg/ml streptomycin (Life Technologies, Belgium) at 37°C in a humidified atmosphere containing 5% CO_2. For in vitro experiments, 2 days after plating (6-well plates; 5.3×10^3 cells/cm^2), COLO205 cells were treated with 5-fluorouracil (3.1, 31 or 310 μM; 5-FU; Fluracedyl, Teva, Belgium), oxaliplatin (0.7 or 7 μM; Eloxatin, Sanofi, UK) or left untreated (control group). For irradiation experiments, tumor cells were irradiated directly in cell culture 6-well plates at room temperature with 2 and 4.5 Gy (XRAD 320, Precision X-Ray, USA) or left unirradiated (control group). Forty hours post chemotherapy and 7, 24 or 48 h post irradiation, COLO205 cells were incubated with ^{99m}Tc-duramycin (0.19 MBq in complete medium) at 37°C for 30 min. After trypsinization, cells were collected by centrifugation (150*g*; 5 min), washed with Dulbecco's Phosphate-Buffered Saline (DPBS), resuspended in fresh RPMI1640 and counted. Cell-bound decay-corrected radioactivity was determined by automatic gamma- (γ) counting (Wizard^2 2480, Perkin Elmer, USA). Radioactivity (counts per minute) per 10^3 cells was calculated and radiotracer binding was expressed as a percentage of the control cells. The levels of drug/irradiation-induced cell death were determined (Muse Annexin V & Dead Cell Assay and Muse Caspase 3/7 Assay, Millipore, USA) for correlation to cell-bound radioactivity.

Animal Model

All the experimental procedures and protocols involving animals are summarized in Figure 1 and were approved by the local ethical committee (2013-36, University of Antwerp, Belgium) and are in accordance with European Directive 86/609/EEC Welfare and Treatment of Animals. CD1-/- nude female mice (aged 6-8 weeks; Charles River Laboratories, Belgium), were subcutaneously inoculated in both hind flanks with luciferase transfected COLO205 cells (2×10^6 in 100 µl DPBS). Baseline and post-treatment tumor volumes were measured daily using a digital caliper, with tumor volumes calculated according to the formula: (length x width^2)/2. Additionally, tumor growth was followed-up using whole-body bioluminescence imaging (BLI).

Approximately 2 weeks after inoculation, the tumors were size-matched (405 ± 40 mm^3), and mice were treated using chemotherapy or radiotherapy. Relative tumor volume was calculated as follows: RTV = (mean tumor volume during treatment)/(mean tumor volume before treatment start). Percentage of tumor growth inhibition was calculated as: %TGI = [1-(mean RTV of treatment group/mean RTV of vehicle group)*100].

Treatment Regimens

For chemotherapy (Fig. 1A), tumor-bearing mice were assigned to 4 treatment groups (n=6 tumors/group): irinotecan (100 mg/kg), oxaliplatin (5 mg/kg), irinotecan (80 mg/kg) in combination with oxaliplatin (5 mg/kg) or the corresponding vehicles (0.9% NaCl or 5% glucose). All the drugs and vehicles were administered by intra-peritoneal injection: irinotecan or oxaliplatin were injected every other day for 1 week and irinotecan was alternated with oxaliplatin for 1 week in the combination therapy. Control tumor-bearing mice received vehicle solution (0.9% NaCl or 5% glucose) on alternating days for 1 week. Treatment-response was assessed by ^{99m}Tc-duramycin SPECT imaging 24 h after the last course of treatment.

To confirm the binding specificity of ^{99m}Tc-duramycin, a blocking study was performed. For this, tumor-bearing mice (n=6 tumors) were treated with irinotecan (80 mg/kg) in combination with oxaliplatin (5 mg/kg), as described above. Unlabeled duramycin (0.1 µg in 0.9% NaCl; Sigma-Aldrich, USA) was injected via the tail vein 30 min prior to ^{99m}Tc-duramycin injection.

For radiotherapy studies (Fig. 1B), prior to tumor irradiation all mice (including mice receiving mock irradiation) were anesthetized with ketamine (80 mg/kg) and xylazine (5 mg/kg), and were positioned on a dedicated tray and the whole body was shielded using lead protection except for the area of the tumor to be irradiated. X-rays were delivered using a self-contained X-ray system (XRAD320, Precision X-Ray, USA) at a rate of 100 cGy/min with 320 KV X-rays. Tumor-bearing mice were assigned to 4 treatment groups (n=5-6 tumors/group), and received a single dose of 4.5 Gy, two fractions of 4.5 Gy in a 24 h interval or pre-treatment with 80 mg/kg irinotecan combined with two fractions of 4.5 Gy in a 24 h interval while in the control group the tumors were not irradiated (mock irradiation). Response to radiation therapy was evaluated 24h after the last treatment.

In Vivo SPECT-Computed Tomography (CT) Imaging

COLO205 tumor-bearing mice received an intravenous injection of ~37 MBq ^{99m}Tc-duramycin via the lateral tail vein, 24 h after the last course of treatment. Static whole-body SPECT images were acquired 4 h post radiotracer injection (p.i.) using a µSPECT-CT scanner (VECTor/CT, MILabs, The Netherlands) equipped with a rat multipinhole SPECT collimator, followed by CT acquisition (45 kV and 615 µA), as described before (*11*). Mice were kept under ~2% isoflurane anesthesia and a constant body temperature during SPECT-CT imaging. SPECT images were reconstructed with ordered-subsets expectation maximization (10 iterations, 16 subsets) and 1.2 mm^3 voxel size, and smoothed with a three dimensional isotropic Gaussian filter of 1.5 mm for visualization purposes. A 20% energy window centered at 140 keV

photopeak was used. CT scans were acquired for attenuation correction and anatomical coregistration with SPECT images. Volumes of interest (VOIs) for the whole tumors, heart (a measure of the blood pool) and muscle (for background measurements) were defined using PMOD v3.3 (PMOD Technologies, Switzerland) based on CT images. ^{99m}Tc-duramycin uptake was quantified from the delineated VOIs as: [total radioactivity concentration in the tumor at the time of scan (kBq/ml)/total radioactivity injected (kBq)] x 100 (%I.D./ml).

Ex Vivo Analysis

After the SPECT-CT scans, mice were euthanized by cervical dislocation for ex vivo biodistribution. After harvesting the tumors, organs and tissues were rinsed in DPBS, weighed and the radioactivity in the samples was subsequently measured in a γ-counter using an energy window of 140 ± 19 keV. Uptake levels of ^{99m}Tc-duramycin were expressed as percentage injected dose per gram of tissue (%I.D./g).

Immediately after γ-counting, tumors were embedded, snap-frozen in tissue-Tek (OCT compound, VWR, USA), sectioned (100 µm) and exposed overnight to phosphor screen plates (Fujifilm, USA). Exposed plates were imaged in a Phosphor Imager system (FLA7000, GE Healthcare, USA). These sections were subsequently stained with hematoxylin and eosin (H&E) following radioactive decay. In addition, adjacent frozen tumor sections (10 µm) were taken at regular intervals across the entire tumor volume, and used for histological analysis of apoptosis. For this, sections were stained with cleaved caspase-3 (CC3, Cell Signaling Technology, USA) and TdT-mediated dUTP nick-end labeling (TUNEL) assay (Promega, USA), according to manufacturer's instructions. For CC3 staining the appropriate horseradish peroxidase-conjugated secondary antibody (DAKO EnVision, Belgium) was used. The nuclei of the tissue sections were counterstained using Mayer's hematoxylin (Sigma-Aldrich, USA). CC3- and TUNEL-positive cells were counted by two independent operators, of which one board-certified pathologist, in a blinded way using an upright microscope at 400x magnification (Olympus

CX31, USA). Three non-sequential whole-tumor sections were analyzed per tumor (n=5-6 tumors/treatment), excluding extensive necrotic areas from the analysis. Apoptosis levels were expressed as the number of apoptotic cells per high power field (HPF; 400x), and correlated to the corresponding radiotracer uptake in the tumor.

Statistical Analysis

Data were expressed as mean ± standard error of the mean. Statistical analysis was performed using Prism v6.01 (GraphPad Software, USA). Statistical differences between different groups were analyzed by the one-way or two-way repeated-measures analysis of variance (time by treatment)#followed by Bonferroni correction. Differences between groups were considered statistically significant if $p<0.05$. For correlation analysis, Pearson's correlation coefficient was computed with $p<0.05$ considered statistically significant.

RESULTS

Cell Binding Assay

Chemotherapy. Upon treatment with increasing concentrations of 5-FU or oxaliplatin, cell death levels were higher in comparison to untreated control cells, as determined by Annexin-V binding and executioner caspase activation (Fig. 2A and Supplemental Fig. 1A, respectively). Accordingly, ^{99m}Tc-duramycin cell binding (Fig. 2B) increased significantly after treatment with 310 μM 5-FU (283.6 ± 27.3%; $p<0.001$; n=6) and 7 μM oxaliplatin (348.2 ± 20.5%; $p<0.001$; n=6), when compared to control (100.0 ± 19.1%; n=6).

Radiotherapy. Temporal ^{99m}Tc-duramycin cell binding was measured at 7, 24 and 48 h post irradiation, as well as the levels of cell death (Fig. 3). High radiotracer binding was evident at 7 h post tumor irradiation, with 146.0 ± 6.0% (n=6) and 142.7 ± 9.8% (n=6) binding after 2 and 4.5 Gy of X-rays, respectively. Significantly lower binding was found in non-irradiated control cells (100.0 ± 10.4%; n=4; $p=0.011$ and $p=0.007$ compared to 2 and 4.5 Gy, respectively). Cell-associated radioactivity was highest at 48 h post 2 Gy (180.1 ± 17.5%; $p=0.043$; n=6) and 4.5 Gy (232.9 ± 25.7%; $p=0.002$; n=6) irradiation (Fig. 3B). Importantly, the levels of cell death were increased in irradiated cells at all the timepoints studied, when compared to control cells (Fig. 3A and Supplemental Fig. 1B) and in good correlation with radiotracer cell binding ($p<0.001$, Pearson's $r=0.76$, 0.80 for annexin-V and caspase-3/7, respectively). A significant increase in necrosis occurred at 48 h after doses of 2 and 4.5 Gy (Fig. 3A).

Evaluation of Treatment Response in Tumors

Chemotherapy. All chemotherapy treatments resulted in a decrease in body weight of less than 20% from the weight at the day of initiation of therapy. Treatment with oxaliplatin did not inhibit tumor growth at day 5 (RTV = 1.62 ± 0.21; $p=0.212$; n=6). On contrary irinotecan resulted in a significant 27.6 ± 5.8% TGI at day 5, which corresponded to a RTV of 1.45 ± 0.11 ($p=0.027$; n=6), when compared to control. Combination therapy (RTV= 1.10 ± 0.19 and 1.18 ± 0.22 at

day 5 and 6, respectively; n=6) further inhibited tumor growth (45.3 ± 10.2%), when compared to control at day 5 (RTV = 1.98 ± 0.24; p=0.002; n=6) and at day 6 (RTV = 2.18 ± 0.19; p<0.001; n=6) (Supplemental Fig. 2A). Similarly, the BLI signal in the tumors of mice treated with irinotecan and combination therapy was significantly lower compared to the vehicle group (Supplemental Fig. 2B). Accordingly, ex vivo γ-counting of excised tumors (Fig. 4A) revealed an increased ^{99m}Tc-duramycin uptake in tumors treated with irinotecan (1.75 ± 0.12%I.D./g; p<0.001) and combination therapy (2.10 ± 0.25%I.D./g; p<0.001), but not in tumors treated with oxaliplatin alone (1.07 ± 0.11%I.D./g; p=0.425), when comparing to vehicle-treated animals (0.74 ± 0.04%I.D./g). Figure 4B shows representative μSPECT-CT images 4 h p.i. of tumor-bearing mice after vehicle or combination therapy. ^{99m}Tc-duramycin distribution was characterized by a high uptake in the treated tumors and a low general background in non-targeted organs (Fig. 4B), with positive tumor-to-blood and tumor-to-muscle ratios (Table 1).

The radiotracer's specificity for cell death was evaluated in a blocking study. Pre-injection of unlabeled duramycin blocked radiotracer uptake in tumors treated with combination chemotherapy (1.09 ± 0.07%I.D./g; p=0.009; n=6), when compared to non-blocked equally treated tumors (2.10 ± 0.25%I.D./g; Fig. 4B). Also, based on the SPECT images semi-quantification, there was no significant difference in ^{99m}Tc-duramycin uptake in the post therapy blocked tumors (0.89 ± 0.09%I.D./ml) versus vehicle treated tumors (0.92 ± 0.06%I.D./ml; p>0.999; n=6).

Radiotherapy. The cell death targeting properties of ^{99m}Tc-duramycin were also evaluated in colorectal cancer-bearing mice treated with radiotherapy (Fig. 5). No body weight loss was observed after radiotherapy. Although radiotherapy did not inhibit tumor growth as determined by caliper measurements (results not shown) and BLI (Supplemental Fig. 2C), radiotracer uptake was increased 24 h after a single-dose of radiotherapy (1.24 ± 0.07%I.D./g; p<0.001; n=6), fractionated radiotherapy (0.87 ± 0.08%I.D./g; p=0.026; n=6) and concomitant fractionated

chemoradiotherapy (0.98 ± 0.06%I.D./g; p=0.004; n=5), when compared to mock irradiated tumors (0.57 ± 0.08%I.D./g; n=6) (Fig. 5B).

Correlation of Radiotracer Uptake to Histology

Radiotracer uptake was correlated to levels of therapy-induced tumor cell death. Drug treated tumors were characterized by the presence of shrunk apoptotic cells with condensed cytoplasm, pyknotic nuclei, and apoptotic bodies, as determined by histochemical analysis (Fig. 6). Tumors of irinotecan (12 ± 1 TUNEL-positive cells; p=0.043 and 11 ± 1 CC3-positive cells; p<0.001; n=6) and combination therapy (14 ± 4 TUNEL-positive cells; p=0.008 and 15 ± 2 CC3-positive cells; p<0.001; n=6) treated mice showed increased levels of apoptosis versus vehicle-treated mice (4 ± 1 TUNEL-positive cells and 2 ± 1 CC3-positive cells; n=6) (Fig. 6B and Supplemental Fig. 3A). Oxaliplatin treatment resulted in a moderate increase in the number of CC3-positve cells (8 ± 1; p=0.014) and did not increase the number of TUNEL-positive cells (8 ± 1; p=0.347; n=6), when comparing to vehicle. Most importantly, the ^{99m}Tc-duramycin uptake in the tumors was highly correlated with the apoptotic response (p<0.001, Pearson's r=0.81 and 0.85 for TUNEL and CC3, respectively). While pre-injection of duramycin blocked radiotracer uptake in tumors treated with combination chemotherapy, the level of apoptotic cells in these tumors was increased (15 ± 1 TUNEL-positive cells; p<0.001 and 14 ± 1 CC3-positive cells; p<0.001; n=6), and similar to non-blocked treated tumors. Autoradiography of the tumors (Fig. 6A, upper panel) showed a regional intratumoral localization of ^{99m}Tc-duramycin and co-localization of cold and hot-spots with tumor areas where there is low and high number of apoptotic cells, respectively (Supplemental Fig. 4). Tracer uptake in the autoradiographs was visibly blocked in tumors of mice pre-treated with duramycin. For irradiated tumors, the levels of TUNEL (9 ± 1 and 8 ± 1 TUNEL-positive cells; p<0.001 for 4.5 Gy and 2x 4.5 Gy, respectively) and CC3-positive cells (5 ± 1; p<0.001 and 4 ± 1 CC3-positive cells; p<0.05 for 4.5 Gy and 2x 4.5 Gy, respectively) were increased compared to the controls (2 ± 1 TUNEL- and 2 ± 1 CC3-

positive cells) and in good correlation ($p<0.001$, Pearson's $r=0.73$, 0.88, respectively) with ^{99m}Tc-duramycin uptake in the tumors (Fig. 7 and Supplemental Fig. 3B).

DISCUSSION

^{99m}Tc-duramycin's in vivo avidity for cell death has previously been demonstrated in animal models of whole-body irradiation and cerebral and myocardial ischemia/reperfusion (*8,10,12*). We recently demonstrated its usefulness in an oncology setting showing ^{99m}Tc-duramycin's ability to early detect irinotecan-induced tumor apoptosis (*11*). In the same study, we showed that the administration of ^{99m}Tc-duramycin is safe from a dosimetry perspective and compatible with SPECT imaging in humans (*11*). The goal of the current study was to further validate its potential for early monitoring of treatment response, using a human colorectal cancer xenograft treated with chemo- and radiotherapy.

We found marked increases in ^{99m}Tc-duramycin uptake in the tumors in 24 h after conventional chemotherapy and radiotherapy regimens, accurately reflecting induction of cell death in the tumors as validated by ex vivo histology. Drug treatment and radiotherapy in vivo induced nuclear condensation, cytoplasm shrinkage and formation of apoptotic bodies, caspase-3 activation and DNA damage in the tumors, as evidenced by H&E, CC3 and clinical gold standard TUNEL staining. The combination of irinotecan plus oxaliplatin induced the highest apoptotic response in the tumors. Importantly, there was a good correlation between ^{99m}Tc-duramycin tumor uptake and histological proof of apoptotic cell death. The increase in ^{99m}Tc-duramycin accumulation in treated tumors versus the vehicle group was in the range of other cell death imaging radiotracers (1.5- to 2.8-fold). For example, in a systematic study where different apoptosis imaging agents are compared, Whitney and colleagues found a 1.4- to 2.1-fold increase in ^{99m}Tc-annexin V and ^{18}F-C-SNAT uptake in lymphoma tumors of mice treated with etoposide (*13*). In our study, the increase in ^{99m}Tc-duramycin uptake was restricted to the tumors, without relevant background in non-targeted organs (*11*). The pharmacokinetic profile of a radiotracer is a decisive parameter for its clinical translation. In the past, ^{99m}Tc-annexin V proceeded to clinical trials where it was used to predict and evaluate tumor response to chemo- (*7,14*) and radiotherapy (*15,16*) in cancer patients. Besides low and non-specific tumor uptake

of ^{99m}Tc-annexin V, these clinical studies showed that this radiotracer was only useful for apoptosis imaging in specific tumor types, such as head and neck squamous cell carcinoma (*15*), and when using cancer therapies that have minor effects on the tumor vasculature like conventional chemotherapy and radiotherapy (*17*). Additional reasons for its failure to reach clinical practice include an inadequate biodistribution profile, with low target-to-background ratio (*18*), as a consequence of the large protein structure of annexin V (36 kDa), and due to almost exhausted chemical alternatives for improvement of the pharmacokinetics of this SPECT tracer. On the contrary, duramycin's small size (2 kDa) warrants ^{99m}Tc-duramycin with a fast blood clearance and low accumulation in non-targeted organs contributing to more optimal imaging properties (*11*).

The specificity of ^{99m}Tc-duramycin to image therapy induced tumor cell death was demonstrated through blocking radiotracer uptake in the tumors with cold duramycin. The ability to displace ^{99m}Tc-duramycin from the PE binding sites in tumors of mice treated with combination therapy supports the specific binding of the radiotracer to PE in apoptotic cells.

Since PE also becomes accessible in necrotic cells due to cell membrane disruption, duramycin might not be able to discriminate between necrotic and apoptotic cell death. Consequently, radiation induced necrosis at 48 h post-cell irradiation might have further contributed to an increase in radiotracer uptake, when compared to earlier timepoints. In vivo, despite the presence of small necrotic tumor areas, radiotracer uptake correlated well with the levels of apoptosis in the tumors. Caspase-3 directed radiotracers might take advantage of the fact that caspase activation is limited to apoptosis, and in this way are specific for apoptosis imaging. However, current challenges include cell entry and efficient accumulation in the cytoplasm. These cell permeability issues have been addressed in the development of a novel apoptosis imaging tracer, ^{18}F-C-SNAT, that undergoes cyclization after cleavage by caspase-3 leading to enhanced accumulation and retention of the tracer in doxorubicin-treated tumors (*19*). This probe has however not been tested in humans and warrants further preclinical testing. Another

class of PET tracers is based on caspase-3 inhibitors, of which one, ^{18}F-ICMT-11, has been pre-clinically evaluated for imaging apoptosis in treated lymphoma, colon, breast (*20*) and lung (*21*) cancer models. Limitations of this class of tracers include low absolute uptake in treated tumors, non-specific binding, due to the high reactivity of the dicarbonyl moiety, metabolic degradation and high abdominal background in the PET images (*22*).

The success of treatment of cancer patients by radiotherapy largely depends on tumor radiosensitivity. The response of a tumor to treatment can vary between individuals because of inherent biological variations such as tumor heterogeneity, availability and accessibility of treatment targets, and expression of genes that govern tumor resistance, host immunologic function, and tumor oxygenation (*23*). In addition, the rate and extent of apoptosis induction depends on the treatment modality, tumor phenotype and treatment protocol applied. Therefore, the optimal timepoint of apoptosis imaging that yields the most predictive information varies accordingly. An increase in ^{99m}Tc-duramycin uptake in the tumors was observed 24 h after the last radiotherapy session, which corresponded to low absolute radiotracer uptake (<1.5%I.D./g) and mild apoptotic response. The good correlation found between radiotracer uptake and the levels of cell death demonstrate the sensitivity of this radiotracer to detect even a minor tumor response to therapy. Nevertheless, as was demonstrated in vitro, the apoptotic response and also ^{99m}Tc-duramycin uptake might increase in a dose- and time-dependent way. Therefore, longitudinal as well as baseline monitoring will be included in further studies.

CONCLUSION

We found increased and specific uptake of ^{99m}Tc-duramycin in apoptotic human colorectal cancer xenografts early after onset of chemo- and radiotherapy. Taken together, the results support the usefulness of ^{99m}Tc-duramycin SPECT imaging as a valuable method for in vivo detection of apoptotic response to anti-cancer therapy. In a clinical context, longitudinal imaging cell death has great significance in the assessment of therapeutic response in

individual patients and has the potential to assist in the design of an optimized cost-effective therapy.

DISCLOSURE

Brian Gray and Koon Pak are employees of Molecular Targeting Technologies, Inc.

ACKNOWLEDGMENTS

This work was supported by GOA (G.0135.13). The authors thank Philippe Joye and Caroline Berghmans for their technical assistance.

REFERENCES

1. Brünner N, Vang Nielsen K, Offenberg H, et al. Biomarkers for therapeutic efficacy. *Eur J Cancer.* 2007;5:129-142.

2. Eisenhauer EA, Therasse P, Bogaerts J, et al. New response evaluation criteria in solid tumours: revised RECIST guideline (version 1.1). *Eur J Cancer.* 2009;45:228-247.

3. Ricci MS, Zong WX. Chemotherapeutic approaches for targeting cell death pathways. *Oncologist.* 2006;11:342-357.

4. Meyn RE, Milas L, Ang KK. The role of apoptosis in radiation oncology. *Int J Radiat Biol.* 2009;85:107-115.

5. Galluzzi L, Vitale I, Vacchelli E, Kroemer G. Cell death signaling and anticancer therapy. *Front Oncol.* 2011;1:1-18.

6. Zeng W, Wang X, Xu P, Liu G, Eden HS, Chen X. Molecular imaging of apoptosis: from micro to macro. *Theranostics.* 2015;5:559-582.

7. Belhocine T, Steinmetz N, Hustinx R, et al. Increased uptake of the apoptosis-imaging agent (99m)Tc recombinant human annexin V in human tumors after one course of chemotherapy as a predictor of tumor response and patient prognosis. *Clin Cancer Res.* 2002;8:2766-2774.

8. Zhang Y, Stevenson GD, Barber C, et al. Imaging of rat cerebral ischemia-reperfusion injury using(99m)Tc-labeled duramycin. *Nucl Med Biol.* 2013;40:80-88.

9. Audi SH, Jacobs ER, Zhao M, Roerig DL, Haworth ST, Clough AV. In vivo detection of hyperoxia-induced pulmonary endothelial cell death using (99m)Tc-duramycin. *Nucl Med Biol.* 2015;42:46-52.

10. Johnson SE, Li Z, Liu Y, Moulder JE, Zhao M. Whole-body imaging of high-dose ionizing irradiation-induced tissue injuries using 99mTc-duramycin. *J Nucl Med.* 2013;54:1397-1403.

11. Elvas F, Vangestel C, Rapic S, et al. Characterization of [99mTc]duramycin as a SPECT imaging agent for early assessment of tumor apoptosis. *Mol Imaging Biol.* 2015;[Epub ahead of print].

12. Wang L, Wang F, Fang W, et al. The feasibility of imaging myocardial ischemic/reperfusion injury using (99m)Tc-labeled duramycin in a porcine model. *Nucl Med Biol.* 2015;42:198-204.

13. Witney TH, Hoehne A, Reeves RE, et al. A systematic comparison of 18F-C-SNAT to established radiotracer imaging agents for the detection of tumor response to treatment. *Clin Cancer Res.* 2015;21:3896-3905.

14. van de Wiele C, Lahorte C, Vermeersch H, et al. Quantitative tumor apoptosis imaging using technetium-99m-HYNIC annexin V single photon emission computed tomography. *J Clin Oncol.* 2003;21:3483-3487.

15. Kartachova M, Haas RL, Olmos RA, Hoebers FJ, van Zandwijk N, Verheij M. In vivo imaging of apoptosis by 99mTc-Annexin V scintigraphy: visual analysis in relation to treatment response. *Radiother Oncol.* 2004;72:333-339.

16. Haas RL, de Jong D, Valdes Olmos RA, et al. In vivo imaging of radiation-induced apoptosis in follicular lymphoma patients. *Int J Radiat Oncol Biol Phys.* 2004;59:782-787.

17. Lederle W, Arns S, Rix A, et al. Failure of annexin-based apoptosis imaging in the assessment of antiangiogenic therapy effects. *EJNMMI Res.* 2011;1:1-10.

18. Blankenberg FG. In vivo detection of apoptosis. *J Nucl Med.* 2008;49 Suppl 2:81S-95S.

19. Palner M, Shen B, Jeon J, Lin J, Chin FT, Rao J. Preclinical kinetic analysis of the Caspase-3/7 PET tracer 18F-C-SNAT for imaging tumor apoptosis after chemotherapeutic treatment. *J Nucl Med.* 2015;56:1415-1421.

20. Nguyen QD, Lavdas I, Gubbins J, et al. Temporal and spatial evolution of therapy-induced tumor apoptosis detected by caspase-3-selective molecular imaging. *Clin Cancer Res.* 2013;19:3914-3924.

21. Witney TH, Fortt R, Aboagye EO. Preclinical assessment of carboplatin treatment efficacy in lung cancer by 18F-ICMT-11-positron emission tomography. *PLoS One.* 2014;9:e91694.

22. Nguyen QD, Smith G, Glaser M, Perumal M, Arstad E, Aboagye EO. Positron emission tomography imaging of drug-induced tumor apoptosis with a caspase-3/7 specific [18F]-labeled isatin sulfonamide. *Proc Natl Acad Sci U S A.* 2009;106:16375-16380.

23. Shiao SL, Ganesan AP, Rugo HS, Coussens LM. Immune microenvironments in solid tumors: new targets for therapy. *Genes Dev.* 2011;25:2559-2572.

FIGURES

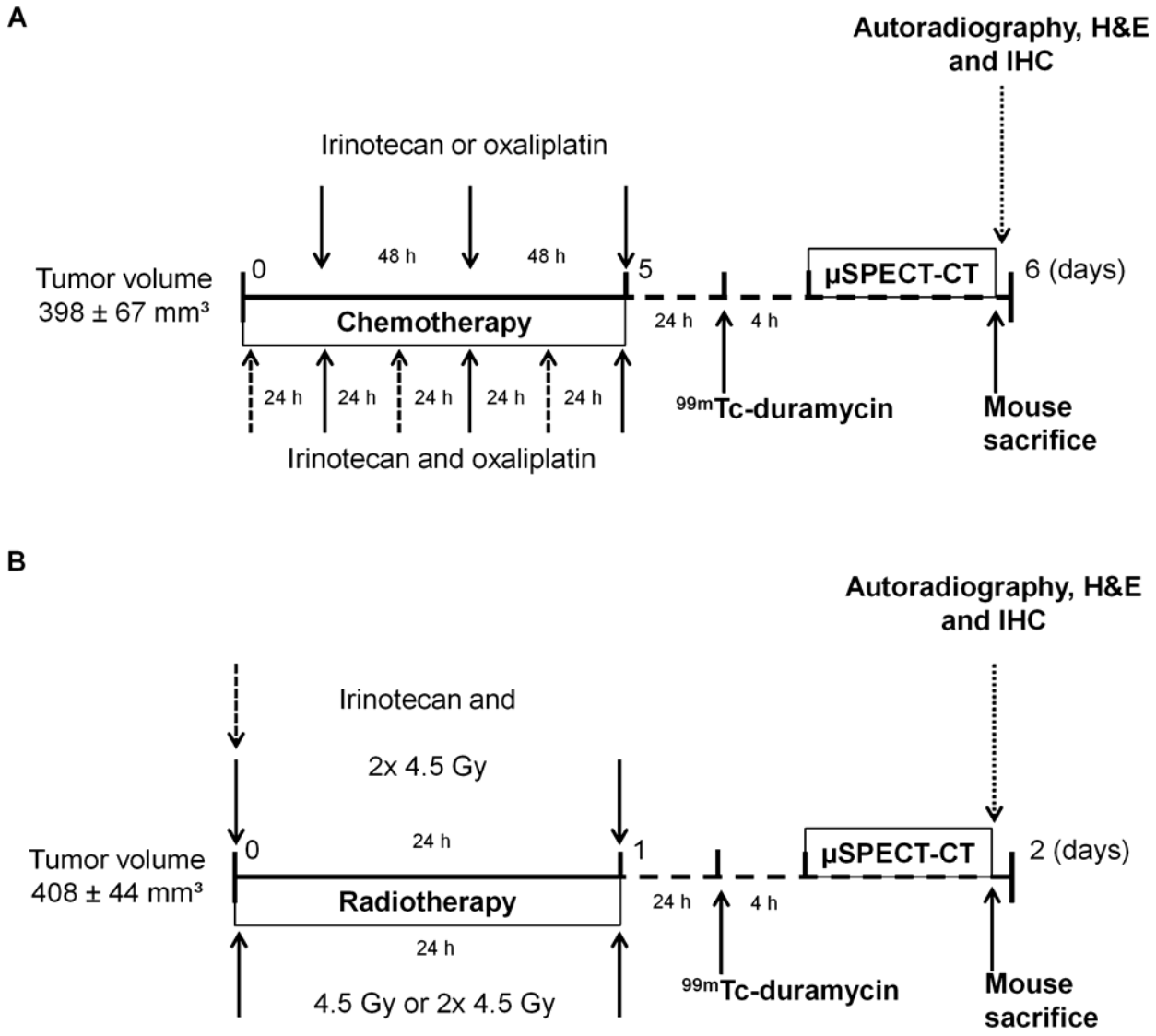

FIGURE 1. Schematic representation of the experimental protocol using ^{99m}Tc-duramycin SPECT imaging in tumor bearing mice treated with (A) chemotherapy or (B) radiotherapy.

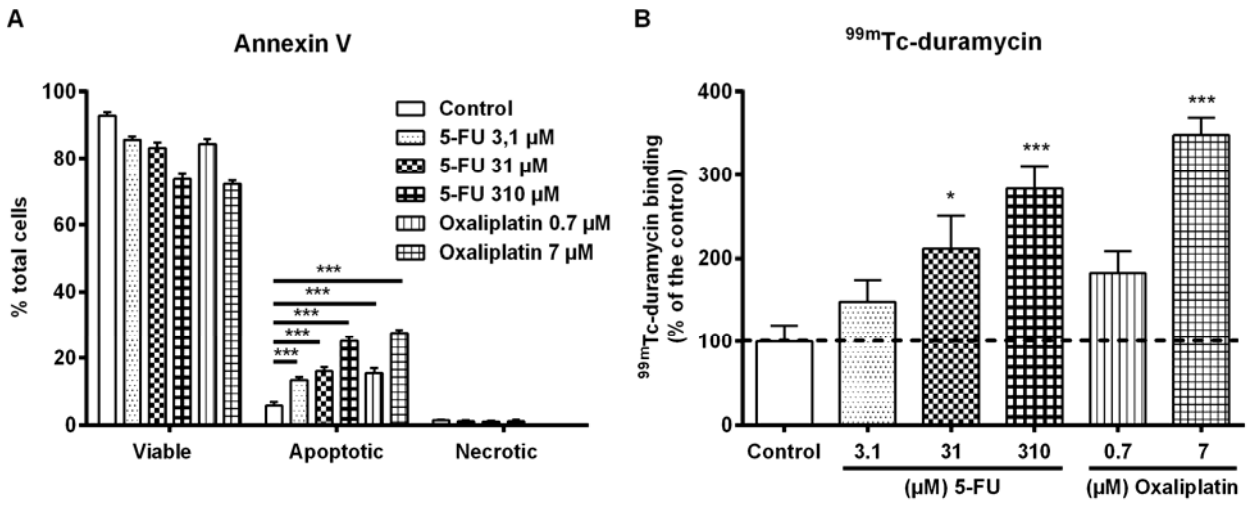

FIGURE 2. Cell death detection in COLO205 cells 40h after treatment with vehicle or chemotherapy by (A) Annexin V assay. (C) In vitro binding of ^{99m}Tc-duramycin. *p<0.05, **p<0.01, ***p<0.001.

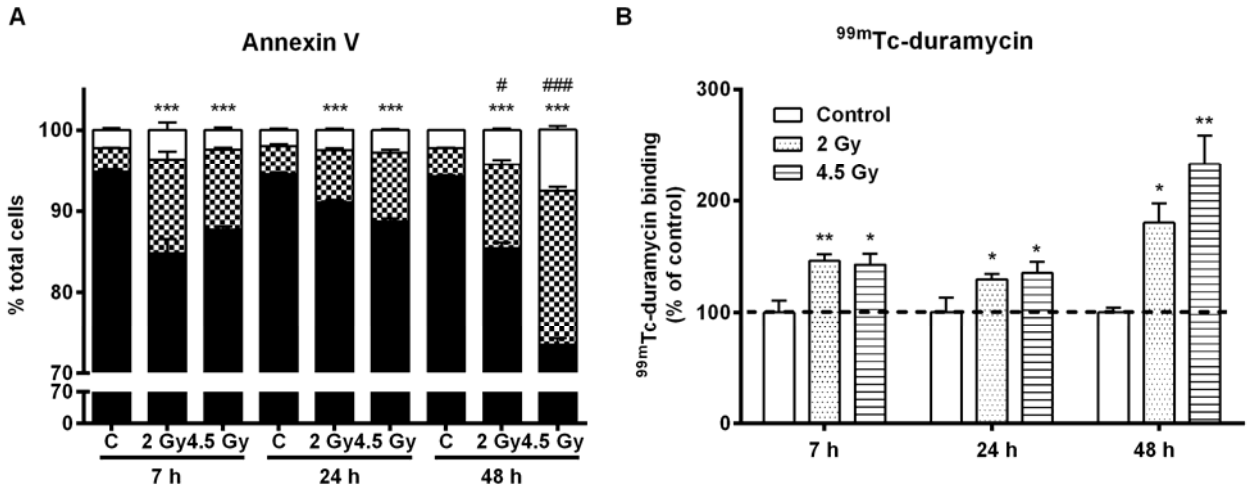

FIGURE 3. Temporal changes in cell death after irradiation measured with (A) Annexin V assay. (B) Time course of ^{99m}Tc-duramycin binding in irradiated and control COLO205 cells. *p<0.05, **p<0.01, ***p<0.001. #p<0.05, ###p<0.001, levels of necrosis significantly different from control.

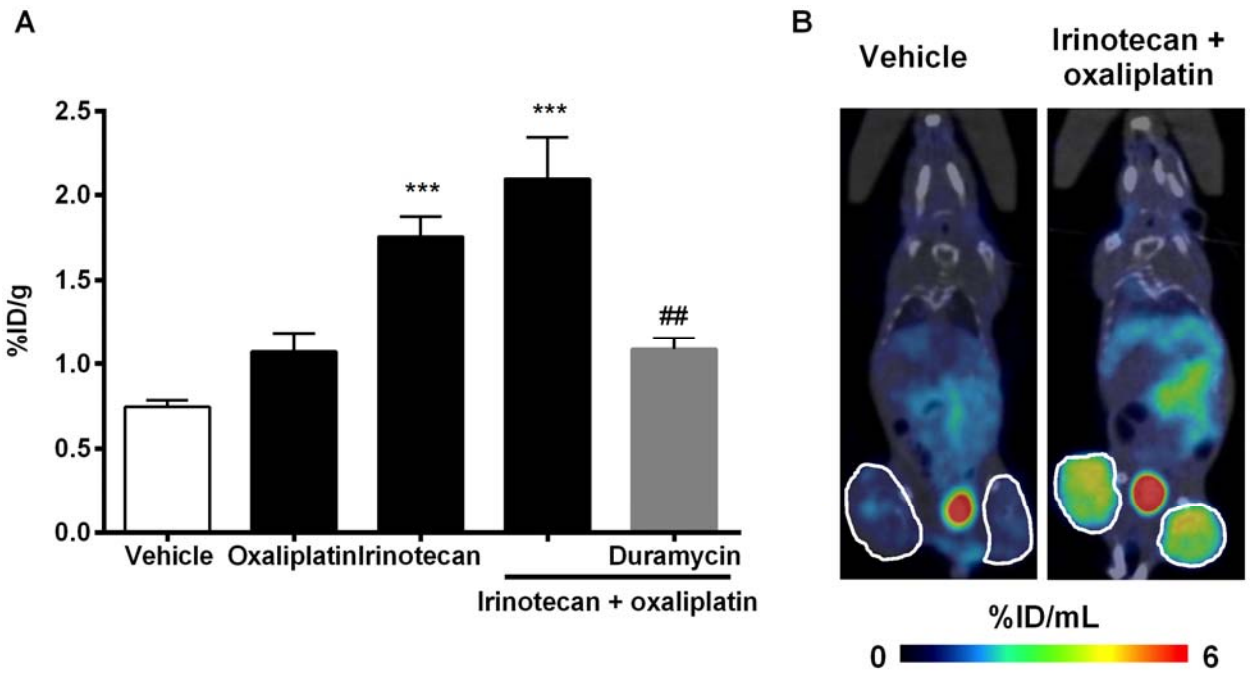

FIGURE 4. Evaluation of ^{99m}Tc-duramycin uptake in tumors treated with chemotherapy. (A) Representative coronal SPECT-CT images showing ^{99m}Tc-duramycin uptake in mice bearing COLO205 xenografts on lower right and left flanks, 24 h after the last course of treatment. Tumors are encircled. (B) Ex vivo ^{99m}Tc-duramycin uptake in the tumors. ***p<0.001, significantly different from the vehicle; ##p<0.01, significantly different from non-blocked tumors.

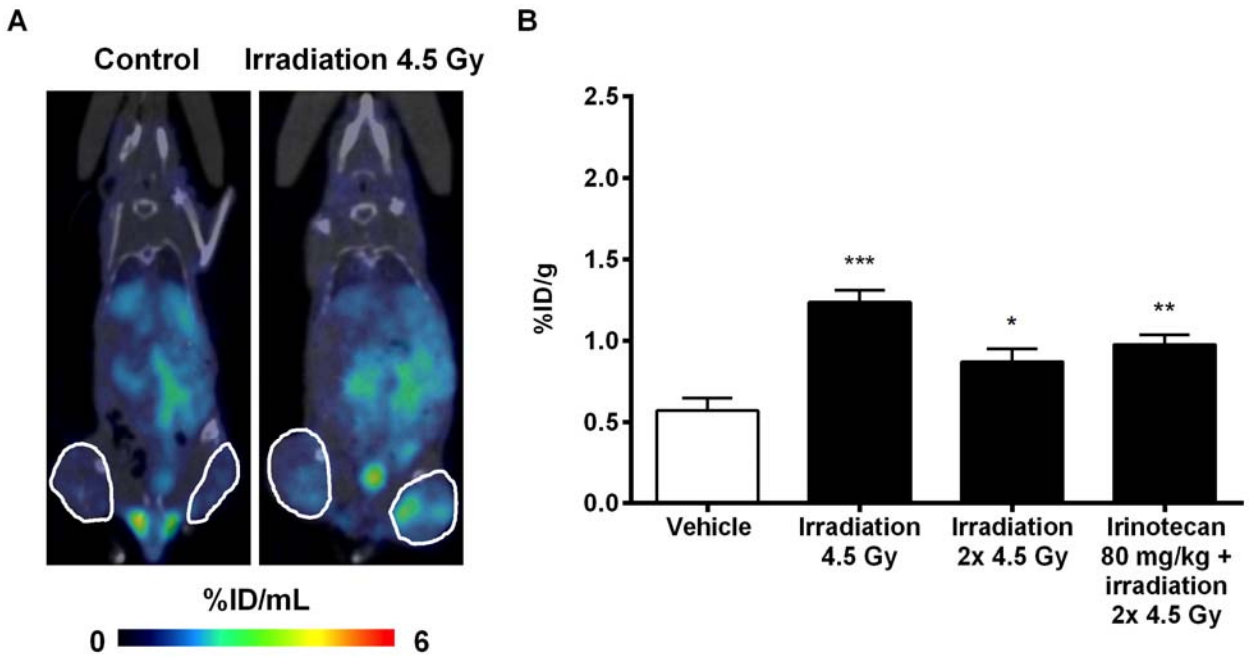

FIGURE 5. Evaluation of tumor response to radiotherapy. (A) Representative coronal SPECT-CT images showing ^{99m}Tc-duramycin uptake in mice bearing COLO205 tumors, 24 h after irradiation. Tumors are encircled. (B) Ex vivo ^{99m}Tc-duramycin uptake in the tumors. *p<0.05, **p<0.01, ***p<0.001.

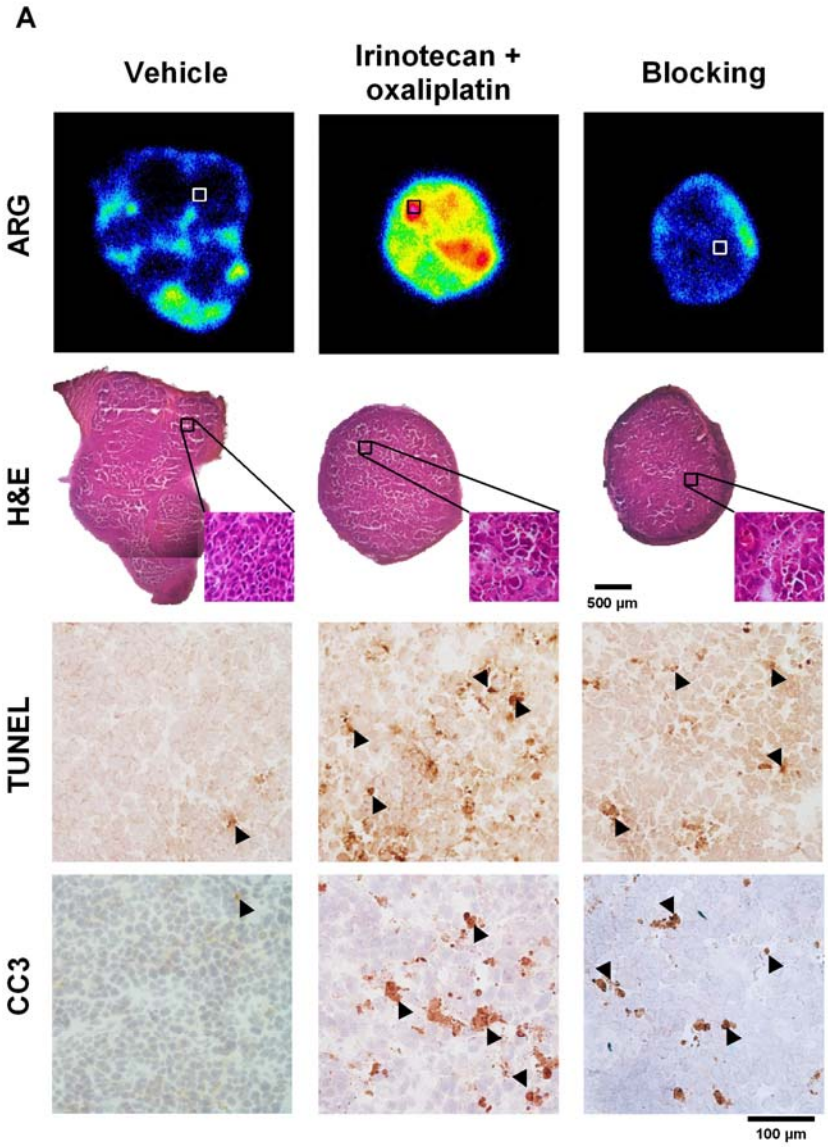

FIGURE 6. Histological and autoradiographic analysis of COLO205 tumors. (A) Representative autoradiography and microscopy images of adjacent histologic COLO205 tumor slices stained with H&E, CC3 and TUNEL. Cells in brown were positive for caspase-3 and TUNEL stainings (arrow heads). Boxes indicate the areas where zoomed images were acquired. Quantitative analysis of the levels of (B) TUNEL-positive cells in the tumors 24h after the last dose. *$p<0.05$, **$p<0.01$. HPF=high power field.

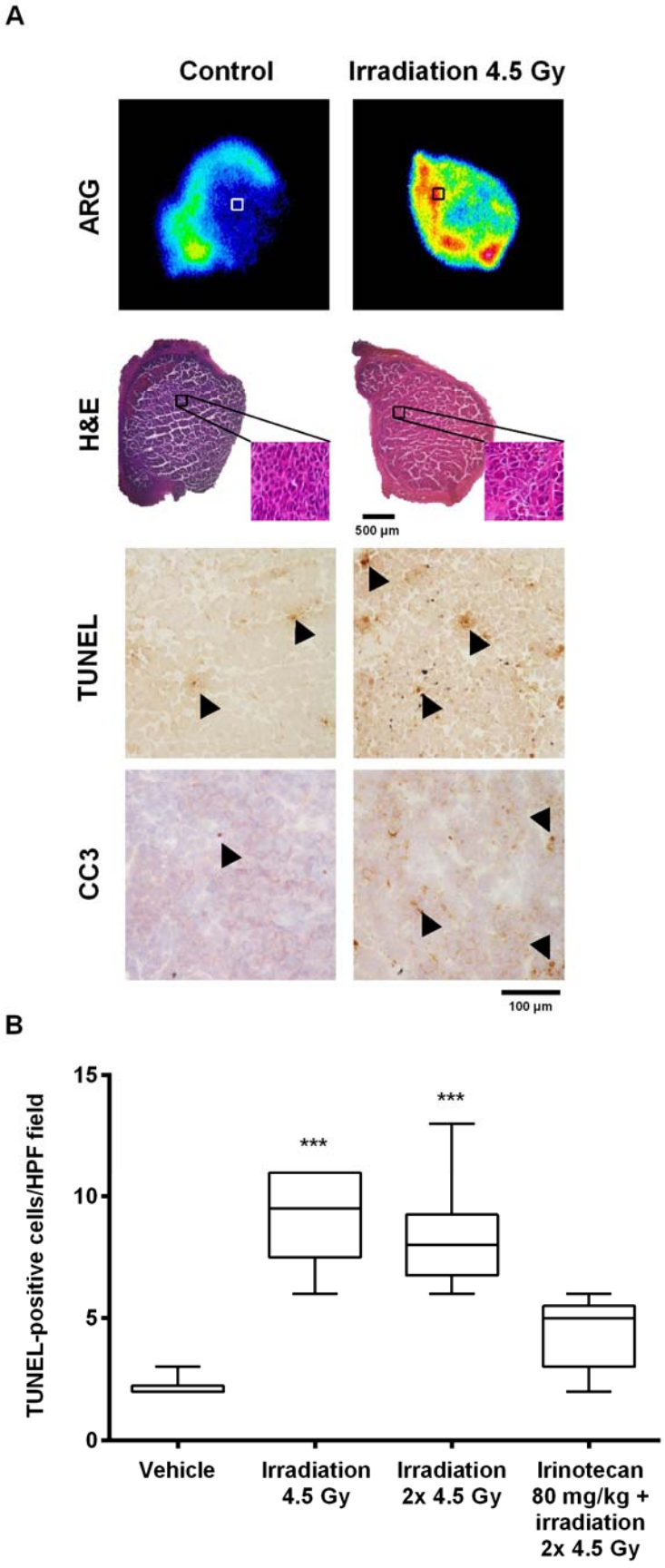

FIGURE 7. (A) Representative autoradiographic and microscopy images of adjacent histologic COLO205 tumor slices stained with H&E, CC3 and TUNEL. Cells in brown were positive for caspase-3 and TUNEL stainings (arrow heads). Boxes indicate the areas where zoomed images were acquired. Quantification of the levels of (B) TUNEL-positive cells in the tumors 24h after irradiation. ***p<0.001. HPF=high power field.

TABLE 1

^{99m}Tc-Duramycin Tumor Uptake and Tumor-to-Background Ratios in Mice Bearing COLO205 Tumors after Chemotherapy

Treatment	^{99m}Tc-duramycin tumor uptake (%I.D./ml)	Tumor-to-muscle ratio	Tumor-to-blood ratio
Vehicle	0.92 ± 0.06	1.6 ± 0.2	1.5 ± 0.2
Oxaliplatin 5mg/kg	1.19 ± 0.12	3.6 ± 0.3	1.6 ± 0.2
Irinotecan 100 mg/kg	1.62 ± 0.07	4.6 ± 0.5	2.4 ± 0.4
Irinotecan 80 mg/kg plus Oxaliplatin 5 mg/kg	2.61 ± 0.46	8.4 ± 0.9	3.4 ± 0.3
Blocking	0.89 ± 0.09	2.0 ± 0.2	1.8 ± 0.2

The Journal of NUCLEAR MEDICINE

Early prediction of tumor response to treatment: pre-clinical validation of ^{99m}Tc-duramycin

Filipe Elvas, Christel Vangestel, Koon Y Pak, Peter Vermeulen, Brian Gray, Sigrid Stroobants, Steven Staelens and Leonie wyffels

J Nucl Med.
Published online: February 2, 2016.
Doi: 10.2967/jnumed.115.168344

The Journal of Nuclear Medicine is published monthly.
SNMMI | Society of Nuclear Medicine and Molecular Imaging
1850 Samuel Morse Drive, Reston, VA 20190.
(Print ISSN: 0161-5505, Online ISSN: 2159-662X)

SNMMI SOCIETY OF NUCLEAR MEDICINE AND MOLECULAR IMAGING